# Alginate foam-based 3-D culture to investigate drug sensitivity in primary leukaemia cells

| | |
|---|---|
| Journal: | *Journal of the Royal Society Interface* |
| Manuscript ID | rsif-2017-0928.R3 |
| Article Type: | Research |
| Date Submitted by the Author: | 27-Mar-2018 |
| Complete List of Authors: | Karimpoor, Mahroo; University College London, mechanical engineering<br>Yebra-Fernandez, Eva; Molecular Pathology, North West London Pathology, Hammersmith Hospital, London<br>Parhizkar, Maryam; Department of Mechanical Engineering, University College London<br>Orlu, Mine; School of Pharmacy, University College London<br>Craig, Duncan Q. M. ; UCL School of Pharmacy, UCL School of Pharmacy<br>Sorouri Khorashad, Jamshid; Molecular Pathology, North West London Pathology, Hammersmith Hospital, London; Centre for Haematology, Department of Medicine, Imperial College, Hammersmith Hospital<br>Edirisinghe, Mohan; UCL, Mechanical |
| Categories: | Life Sciences - Engineering interface |
| Subject: | Biomaterials < CROSS-DISCIPLINARY SCIENCES |
| Keywords: | Scaffold, Leukaemia, three-dimensional, culture, drug resistance |

**SCHOLARONE™**
Manuscripts

# Alginate foam-based 3-D culture to investigate drug sensitivity in primary leukaemia cells

Mahroo Karimpoor[1,2,3], Eva Yebra-Fernandez[4], Maryam Parhizkar[1], Mine Orlu[3], Duncan Craig[3], Jamshid S Khorashad[2, 4] Mohan Edirisinghe[1]

[1]*Department of Mechanical Engineering, University College London, Torrington Place, London, WC1E 7JE, UK*
[2]*Centre for Haematology, Department of Medicine, Imperial College, Hammersmith Hospital, Du Cane Road, London, W12 0NN, UK*
[3]*School of Pharmacy, University College London, 29-39 Brunswick Square, London, WC1N 1AX, UK*
[4]*Molecular Pathology, North West London Pathology, Hammersmith Hospital, London, W12 0HS, UK*

**Running heads**: Porous alginate foam scaffold for antileukaemia

**Correspondence:**

Professor Mohan Edirisinghe
m.edirisinghe@ucl.ac.uk

409 Roberts (Engineering Building), Torrington Place, London, WC1E 7JE.
Tel: 00442076793942,  Ex: 33942
Fax: 00442073880180

**Abstract**

Development of assays for evaluating the sensitivity of leukaemia cells to anti-cancer agents is becoming an important aspect of personalized medicine. The conventional cell cultures lack the three-dimensional (3D) structure of the bone marrow, the extracellular matrix and stromal components which are crucial for the growth and survival of leukaemia stem cells. To accurately predict the sensitivity of the leukaemia cells in an *in vitro* assay a culturing system containing the essential components of bone marrow is required. In this study, we developed a porous calcium alginate foam-based scaffold to be used for 3D culture. The new 3D culture showed to be cell compatible as it supported the proliferation of both normal hematopoietic and leukaemia cells. Our cell differential assay for myeloid markers showed that the porous foam-based 3D culture enhanced myeloid differentiation in both leukaemia and normal hematopoietic cells compared to 2D culture. The foam-based scaffold reduced the sensitivity of the leukaemia cells to the tested antileukemia agents in K562 and HL60 leukemia cell line model and also primary myeloid leukaemia cells. This observation supports the application of calcium alginate foams as scaffold component of the 3D cultures for investigation of sensitivity to antileukaemia agents in primary myeloid cells.

**Key words**: Scaffold; Leukaemia; three-dimensional, culture, drug resistance

## 1.Introduction

The bone marrow (BM) niche is a specialized microenvironment where stem cells reside. The niche is believed to regulate stem cell quiescence, self-renewal and differentiation[1]. There are several components that regulate the function of the niches [2-4]. These factors include cellular components such as osteoblast, osteoclasts, endothelial cells, mesenchymal progenitors and molecules such as stromal derived factor1 (SDF-1), stem cell factor, osteopontin, thrombopoietin and N-cadherin[5].

Traditionally monolayer cell culture has been used for studying hematopoietic stem cells (HSC) but they are not capable of producing a niche like structure and therefore have not been suitable models for this purpose[6]. Considering the deficiencies of current two-dimensional cultures[7], recent efforts has focused on developing 3D cultures which can mimic BM microenvironment by accommodating the essential components of the BM. The cultures with only cellular and cytokine components without providing the 3 dimensional structure have been able to support the expansion of the more differentiated hematopoietic precursor CD34^{+} cells without establishing a support for long-term HSC self-renewal[3]. A lack of 3D structure and molecular matrix components are potential causes of their unsustainability for long-term HSC culture[8]. Molecules present in the 3D structure have significant impact on making the culture more similar to BM niches including segment-1(CS-1) and RGD motifs which mimic the fibronectin domains of the extracellular matrix (ECM) and contribute to expansion of CD34^{+} cells[9].

The development of an *ex-vivo* 3D culture mimicking the BM microenvironment in providing niche-like structures for the HSC to reside and proliferate provides an opportunity to study hematological malignancies. The acute myeloid leukaemia (AML) cells have a subpopulation called leukaemia stem cells (LSC) which has the capacity to initiate the disease and continue producing leukaemia cells and also perform self-renewal. The main challenge for studying

3

AML cells for therapeutic target discovery purposes has been the difficulty in growth and maintenance of these cells in an *in vitro* culture[10]. The majority of AML cells usually undergo spontaneous apoptosis and only a subpopulation of the cells proliferate during *in vitro* culture[11]. The proliferation and survival of the AML cells increases in the presence of hematopoietic growth factors, co-culture with stromal cells and a 3-dimensional environment[10-12]. It has also been shown that AML cells have reduced sensitivity to chemotherapeutic agents in 3D cultures[13]. Insufficient information on molecular interaction between the AML LSCs and their microenvironment is one of the main reasons for failure of current therapeutic approaches[14]. The new approaches should be focused on selectively inhibiting LSC by disrupting the interaction between them and their niche environment but at the same time preserving the normal haematopoiesis. Long term low level *BCR-ABL* oncogene detection by sensitive PCR techniques in CML patients who achieve major molecular response to tyrosine kinase inhibitors is believed to be due to the survival of LSC in the BM niches in spite of the inhibition of BCR-ABL kinase activity[15].

A 3D culture mimicking BM microenvironment provides a model through which the mechanism of LSC maintenance can be explored and this facilitates the investigations toward developing drugs targeting the survival pathways activated by such interactions. Various 3D cultures have been developed so far for studying leukaemia cells. We have already developed PMMA-HA fibre-based scaffold to show the influence of 3D culture on reduced sensitivity of leukaemia cells to the tested antileukaemia agents[16]. The PMMA-HA scaffold provides a 3D structure and by having hydroxyapatite (HA) simulate some characteristics of the bone however, it lacks the spongious structure of the BM. To develop a scaffold with pores similar to bone lacuna we developed in this work, a foam-based scaffold with spongious structure using alginate biomaterial[17, 18]. Microbubble technology was applied to produce the foam with the expected size of the pores[19]. This foam-based 3D culture supported the growth of

4

normal haematopoietic and also leukaemia cells, and similar to *in vivo* condition it promoted

cell differentiation. This system reduced the sensitivity of the leukaemia cells to

antileukaemia agents. Due to simulating the physiological condition our foam-based scaffold

can be used for drug sensitivity studies of the primary leukaemia cells.

## 2.Results

### 2.1. Material and solution characteristics

In the process of microbubble production using a microfluidic technique, parameters such as

gas pressure, liquid flow rate and viscosity have a significant influence on the diameter size

of the bubble and their formation in the V-junction device (Figure S1a). Monodisperse

microbubbles with average diameter 150μm were obtained at gas pressure of 95-120 kPa and

obtain flow rate of 200-250 μl/min. In this study to improve the stability of alginate

microbubbles, they were collected in 2% wt. calcium chloride solution to cross-link the

bubbles shell. This made the shell stronger and as a result the bubbles lasted longer and

allowed time for the foam structure to evolve (Figure S1b). Physical properties such as

viscosity and surface tension have significant impact on the bubble formation process. In the

current study, the surface tension of alginate-PEG liquid was measured to be 49 mN/m, using

a Kruss Tensiometer (Model-K9, Kruss GmbH, Germany). The viscosity was measured to be

20 mPa s, using a Brookfield DV-11 Ultra programmable Rheometer (Brookfield

Engineering Laboratory Inc., Middleboro, MA, USA). To obtain accurate results different

measurements were performed at ambient temperature (22 °C) and the average of seven

readings was taken to ensure accuracy.

### 2.2. Foam-based scaffold

Foams are metastable inclusions of gas in a fluid phase and are frequently used in the food

industry and biomedical applications. In this study, solid foam structures with high porosity

5

were successfully prepared by cross-linking the alginate microbubbles (Fig 1). The foam

scaffold was dried (as observed by optical microscopy) after 10 days of incubation in a

desiccator.  Foam scaffolds showed typical ladder-like porous structure with porous size

ranging between 20 and 200 μm (Figure 1).

### 2.3. Bioactivity and biocompatibility of scaffold

To allow cell growth and support biocompatibility features, it is critical that the scaffolds

have high porosity and bioactive nanoparticles are incorporated in them. Hydroxyapatite

(HA) is the main inorganic component of bone material and is widely used in various

biomedical applications due to its excellent bioactivity and biocompatibility. In this study to

support cell compatibility, HA nanoparticles (diameter<200nm, 5% wt.) were added to the

scaffold structure. This was achieved by adding the HA to the alginate solution prior to

forming bubbles using the v-junction. We observed settlement of K562 and primary AML

cells in the microcavities of the scaffold which is an evidence for the biocompatibility of the

prepared foams (Figure 2). The cells were concentrated in the microcavities and around the

scaffolds indicating the attraction of this scaffold to the leukaemia cells.

### 2.4. Differentiation of the primary haematopoietic cells and acute myeloid leukaemia cells

Mononuclear cells from a newly diagnosed AML patient were cultured in the presence and

absence of scaffold (in triplicate). The cell counts after 5 days of culture showed larger

number of AML cells in the scaffold compared to no scaffold (Figure S2) this supported the

cell friendly nature of the alginate scaffold. To investigate whether the scaffolds influence the

differentiation of the leukaemia and normal stem/progenitors, the myeloid differentiation of

the CD34^{+} cells from one normal and two AML patients were investigated in the presence or

absence of foam scaffolds for 3 days. The antigenic expression of primary normal

haematopoietic cells (Figure 3A) and two different acute myeloid leukaemia cells (Figure 3B

6

and 3C) from day 0 to 3 was measured by flowcytometry. Normal CD34$^+$ precursors showed stronger and more homogenous expression of the myeloid associated antigens CD117 and CD13 after 3 days culture in the foam-based scaffold compared to non-scaffold (2D) culture indicating enhanced differentiation. Similarly, in figure 3B, myeloblasts had augmented intensity of HLA-DR and CD13. This was even more evident in figure 3C, where the blasts showed a profound monocytic differentiation compared to 2D culture, having stronger expression of HLA-DR and CD11b. Enhanced differentiation of CD34$^+$ cells to more differentiated cells (represented as reduced CD34$^+$ expression) was also observed in myeloblasts from the third AML patient (Figure S3). The findings from this observation suggest that foam-based 3D culture enhances myeloid differentiation in the normal CD34$^+$ cells and also myeloblasts from AML patients. Further information on the expression of the markers for patients in figure 3 is provided in supplementary information (Table S1 and figure S4).

### 2.5. Resistance of the CML and AML cells to inhibitory effect of the drugs

Using different types of scaffolds, we showed previously[16] that 3D cultures reduced the sensitivity of leukaemia cell lines to antileukaemia agents. Due to lack of prior knowledge about the potential level of resistance which might be induced by the foam scaffold, we investigated various inhibitory concentration of imatinib or doxorubicin for K562 or HL60 and HS-5 cells. In our earlier work, we determined the lowest inhibitory dose of imatinib for K562 to be 0.5μM[16]. To determine the lowest inhibitory dose of doxorubicin for HL60 cells which is not toxic to HS-5 stromal cells, both cell lines were treated with various doses of doxorubicin followed by MTS assay. This experiment identified 0.1 μM as the lowest inhibitory dose of doxorubicin for HL60 which had no inhibitory effect on HS-5 cell co-culture (Figure 4). To investigate the potential drug-resistance mediated by the foam-based

scaffold, K562 and HL60 cells were treated with imatinib and doxorubicin, respectively. Treatment of K562 or HL60 cells in foam-based 3D culture reduced their sensitivity to imatinib or doxorubicin, respectively (Figure 5 a, b). As stroma is an important component of BM microenvironment, to assess the sensitivity of leukaemia cells to antileukaemia agents in the context of stromal cells, BM-derived HS-5 stromal cells were seeded to the foam-based scaffold. For HL60 cells, addition of HS-5 cells further reduced the sensitivity of HL60 to 0.1μM doxorubicin (Figure 5b). Although addition of HS-5 cells to foam scaffolds increased the trend toward resistance, K562 cells treated with 0.5 or 1 μM imatinib, the difference was insignificant (Figure 5a). The lack of any trend toward resistance in the co-culture of HL60 and HS-5 in foam-based scaffold compared to no HS-5 condition might be due to inhibitory dose of doxorubicin on HS-5 at doses higher than 0.1μM doxorubicin (Figure 5b). To show primary leukaemia cells behave similarly, primary myeloblasts from an AML patient were cultured in the presence or absence of foam-based scaffolds and treated with or without doxorubicin (0.1, 0.2 and 0.4μM) followed by cell proliferation and viability using MTS assay at 72 hours. Foam-scaffolds reduced the sensitivity of AML cells to doxorubicin at 0.2 and 0.4 μM (Figure 5c). The lack of difference at 0.1μM seems to be the lower sensitivity of primary AML cells to doxorubicin compared to HL60 cells.

## 3.Discussion

Tissue engineering scaffolds play an important role in biomedical applications by acting as a temporary tissue construct or building block for cell accommodation, proliferation and differential function[20]. In the current study foam scaffolds were prepared by a microfluidic bubbling technique. To overcome the poor stability of the microbubbles which is a limitation of this technique crosslinking by calcium chloride was practiced [21]. To improve biocompatibility of the scaffold, porous foam was fabricated from natural polymer alginate.

8

To improve cell seeding and growth recently many attempts have been made such as coating the scaffolds with different proteins like collagen and FBS[22-24], here we used HA nanoparticles to make the scaffold more similar to bone marrow microenvironment for biological investigations.

To develop a bone marrow like environment with niche like structures we formed foam-based scaffolds derived from microbubbles. Application of this technology has the advantage of controlling the size of the microbubbles and as a result controlling the size of the microcavities in the foam. This enabled production of scaffold with pores of about 200μm in diameter, which is close in size to the microcavities in the bone [25, 26]. The challenge for using this technology to produce foamed scaffolds is the instability of the produced bubbles which results in destruction of bubbles before forming solid foam during drying. To overcome this problem, we collected microbubbles in calcium chloride solution which caused cross links in the microbubble shell and the formation of solid foam following drying. The images from these scaffolds showed the production of desired microcavities and validates the use of this approach for production of foam-based scaffold.

One of the main purposes of developing artificial bone marrow like structures for culturing leukaemia cells is drug sensitivities[27]. Foam-based 3D culture similar to fiber scaffolds[16] increased the resistance of the leukaemia cell lines to inhibitory effects of imatinib and doxorubicin. Different applied materials in the structure of the fiber and foam-based scaffolds and observation of similar phenotypes in K562 and HL60 cells in response to imatinib and doxorubicin suggest the 3D environment and interaction of the leukaemia cells at different spatial positions has an important influence on their survival and activated signaling pathways, and as a result response to antileukaemia drugs. It has been shown before that 3D cultures influence the cell phenotype and their gene expression compared to 2D environment

9

[28]. This altered phenotype might be due to activation of another signaling pathway which is targeted by the inhibitor. The other possibility is the altered oxygen concentration in 3D compared to 2D culture. Hypoxia is an important component of the BM niche and contributes to the maintenance of AML cells[29, 30] and also selects bortezomib-resistant CML stem cells[31]. It has been shown that 3D-cultures are better than 2D-cultures in simulating important tumor characteristics *in vivo* such as hypoxia and resulting drug resistant phenotype[32]. The mechanism of resistance might also be due to poor access of drugs to the cells hidden in the niche like spaces in the scaffold. These provide more evidence for the application of 3D culture for drug sensitivity studies. Conventional 2D cultures have been proven to be an unreliable drug development model for prediction of *in vivo* drug efficacy and toxicity[33]. Creating a third dimension for cell culture is clearly more relevant and has to be considered as a practical alternative[34].

Our data showed enhanced myeloid differentiation in both normal progenitor and AML myeloblasts in 3D foam-based culture. 3D cultures have also been reported in other studies to be capable of inducing differentiation of the hematopoietic stem cells compared to 2D cultures[35, 36]. 3D cultures mimic an environment to *in vivo* bone marrow niches compared to 2D inducing cell differentiation[37]. Although this observation does not address directly how this can influence resistance to therapeutic agents it might suggest that 3D culture causes higher resistance to antileukaemia agents compared to 2D cultures by inducing higher differentiation rate and production of the more mature cells which are less sensitive to inhibitory effect of antileukaemia agents. As resistance or relapse in AML is considered to be mainly due to the role of LSC, future investigations should aim at measuring the impact of 3D cultures on LSCs and if 3D culture affects the self-renewal activity of LSCs. In summary, the conventional 2D culture is not a highly reliable system for drug sensitivity investigations as the drug sensitivity of leukaemia cells obtained from 2D culture is different from what is

10

observed *in vivo*[38]. Our foam-based 3D culture reduced the sensitivity of leukaemia cells to antileukaemia agents and further induced the differentiation of the normal and leukaemia cells compared to 2D culture. These differences might be attributed to microcavities mimicking bone marrow niches in foam-based 3D culture. We propose to apply this foam-based 3D culture for drug sensitivity investigations and therapeutic target discoveries.

## 5.Conclusions

Recent developments in understanding the role of bone marrow microenvironment in the formation and progress of various myeloid leukaemia has created a new opportunity for development of novel therapeutic approaches. Targeting the interaction between the leukaemia cells and the microenvironment is expected to eradicate leukaemia cells residing in the bone marrow niches. Mesenchymal stromal cells, osteoblasts and extracellular matrix are among the main components of the bone marrow microenvironment whereby their special 3D organization contributes to the formation of niches. This is a very different structure compared to conventional 2D cultures which have been used extensively for measuring the sensitivity of the leukaemia cells to various antileukaemia agents. Our investigations have shown that a higher level of resistance to antileukaemia agents is induced by 3D culture mimicking bone marrow compared to 2D culture and support the application of 3D culture as the in vitro model to investigate the drug sensitivity. This has been achieved by using an alginate foam-based scaffold prepared using microbubbles generated by a microfluidic device.

## 6.Experimental Section

### 6.1. Solution preparation

All the polymers in this study were purchased from sigma-Aldrich (Poole UK) unless stated otherwise. To prepare the aqueous alginate solution, 1% wt. sodium alginate powder was

11

dissolved in deionized water followed by the addition of 0.5% wt. polyetheyleneglycol-40

(PEG- 40S, Sigma-Aldrich, Poole, UK, density; 1300 kg/m$^3$) as a surfactant. The mixture

was stirred using a magnetic stirrer (KIKA, Labor-Technology RCT basic stirrer) for two

hours to allow for even dispersion of the compounds. 0.5% wt. of Phospholipid

(hydrogenated powder) was weighed and added to the solution followed by further stirring

for approximately another 2 hours until a homogenous solution was obtained.

### 6.2. Microfluidic Process

A V-junction microfluidic set-up is illustrated in figure S1a. It was used to generate

monodisperse microbubbles[19]. The V- junction microfluidic device is fabricated using

poly(methylmethacrylate) via CNC machining. It consists of three Teflon capillaries with a

constant inner diameter (200 μm). The vertical capillary is connected to a gas cylinder, via a

digital manometer for controlling the pressure supplied to the junction. The sides deck

capillaries provide solutions flow and are connected to a syringe via a syringe pump

(Harvard, PHD 4400). To generate microbubbles, the gas pressure was gradually increased

until it overcame the surface tension of the supplied alginate solution. The liquid and gas

from all three capillaries met at the intersection zone of the junction. This produced bubbles

at the gas–liquid interface from the bottom inlet. The bubbles were deposited into arrays

which dried naturally to give the foam samples. The temperature and relative humidity during

processing was 21 °C and 40 to 60 % respectively.

### 6.3. Foam sample analysis

The microbubbles size and uniformity were examined using an optical microscope (Zeiss

Axiotech) fitted with a Nikon Eclipse ME 600 camera. Foam scaffold morphology was

assessed using a Jeol JSM-6301F field emission scanning electron microscope (FE-SEM,

JEOL Ltd., Herts, UK). Prior to imaging examination, the samples were coated with 20nm of

12

gold under argon using Quorum Q150T Turbo-Pumped Sputter Coater. All the SEM images were taken at an acceleration of voltage of 5kV with a working distance of 15–35 mm. The average microbubble diameter was determined by measuring their diameter at ~ 50 points in the SEM images using the ImageJ software (Version 3.00).

### 6.*4. Preparation of Normal Hematopoietic and Acute Myeloid leukaemia cells*

Mononuclear cells (MNCs) were separated by density centrifugation on Ficoll-Hypaque (Nycomed, Zürich, Switzerland) from peripheral blood of newly diagnosed AML and CML patients and cryopreserved. Informed signed consent was obtained from the patients for using their samples for research. The samples were approved for research under Imperial College Tissue Bank ethical approval for myeloid leukaemia research. Prior to use in assays, fresh or frozen CD34$^+$ cells were cultured in StemSpan SFEM supplemented with cytokines (CC100; StemCell Technologies) for 24-48 h at 37$^o$C. The donor gave informed consent for research application of the sample.

### *6.5. Cell culture*

For 2D culture, K562, AR230 and HL60 cell lines were cultured in RPMI medium supplemented with 10% FBS, 2 mM L-glutamine and 100 U/mL penicillin/streptomycin (RF10). The cells were cultured at a concentration of 25e4/ml. For 3D culture, the prepared scaffolds were transferred to 24-well culture plates and sterilized by exposure to ultraviolet light for 2 hours followed by washing three times with PBS. After the third wash, 1 ml of RF10 was added to each well followed by incubation of the plates at 37 °C in a cell culture incubator for 24h. Subsequently, the medium was removed. Primary AML cells, K562 or HL60 cell lines were suspended at 25 x 10$^4$/ml concentration and then 1ml of the cell suspension was added to each well. For the drug sensitivity study, a final concentration of

13

0.5, 1 or 2 µM imatinib or 0.1, 0.2 or 0.4 µM doxorubicin was used. The experiments were done in triplicate for the control and treated condition and were carried out twice.

### 6.6. Co-culture of HS-5 with Leukaemia cells

Foam-based 3D culture was developed by adding HS-5 cells to calcium alginate foam scaffolds. 15 x $10^4$ GFP$^+$HS-5 cells were suspended in 1ml RF10 and transferred to each well of the plates containing the scaffold foam. 24 hours later 5 x $10^5$ K562 or HL60 cells were added to each well. After another 24 hours, the drug treated groups were given 0.5 or 1 µM imatinib or 0.1 or 0.2 µM Doxorubicin. 72 hours later, the live K562 or HL60 cells were counted using Countess II FL (Life technologies, USA). Each condition was done in triplicate and the experiment was done twice. Similar approach was applied to primary AML cells.

### 6.7. Differentiation of the cells using Flowcytometry

CD34$^+$ cells from one normal and two AML patients were cultured in StemSpan (Thermofisher) supplemented with CC100 (StemCell Technologies) in foam-based 3D and 2D culture. Myeloid markers were measured at the time of culture and then re-assessed after 3 days. To retrieve the cells, the supernatant was removed from the 3D culture followed by washing the scaffold with PBS and then treating the scaffold with Trypsin-EDTA (Sigma-Aldrich). After 5 minutes of incubation at 37$^o$C the supernatant was removed and passed through filter. Immunophenotype was determined using 8-color Euroflow AML/MDS antibody panel tube 1 (CD16 FITC, CD13 PE, CD34 PerCP-Cy5.5, CD117 PE-Cy7, CD11b APC, CD10 APC-H7, HLA-DR V450, CD45 V500). Data was acquired in a BD FACSCanto II flow cytometer (BD) and analysed with Infinicyt software (Cytognos).

### 6.8. MTS Assay

Cells ($10^4$) were suspended in 200 µL medium ± inhibitor and cultured in triplicate in a 48-well plate in the presence or absence of inhibitors (imatinib or doxorubicin) at indicated concentrations. Following 72 hours, CellTiter 96 AQueous One Solution MTS Reagent (Promega) was added according to the manufacturer's instructions. 100 µL of the medium was transferred from each well to 96-well followed by measuring the dye absorbance at 490 nm using Multiskan GO Microplate Spectrophotometer (ThermoFisher Scientific).

### 6.9. Statistical analysis

All the statistical analysis was done using Graphpad prism software version 7. A 2-tailed Student $t$ test was used for assays with cell lines and primary cells. For 3-(4,5 dimethylthiazol-2-yl)-5-(3-carboxymethoxyphenyl-2-(4-sulfophenyl)-2H-tetrazolium (MTS) assays, 3 independent experiments each with 3 replicates per concentration were performed on unique plates with untreated controls.

### Authors' contributions

MK carried out the lab work, participated in data analysis, design the study and drafted the manuscript; EYF, MP participated in data analysis, MO, DC reviewed the data and commented on the manuscript, JSK designed the study, reviewed the data, coordinated the study and helped draft the manuscript, ME, coordinated the study and helped draft the manuscript. All authors gave final approval for publication.

### Acknowledgment

### Conflict of Interest

The authors declare no conflict of interest.

## References

[1] Schofield, R. 1978 The relationship between the spleen colony-forming cell and the haemopoietic stem cell. *Blood Cells* **4**, 7-25.

[2] Fraser, C.C., Eaves, C.J., Szilvassy, S.J. & Humphries, R.K. 1990 Expansion in vitro of retrovirally marked totipotent hematopoietic stem cells. *Blood* **76**, 1071-1076.

[3] Haylock, D.N., To, L.B., Dowse, T.L., Juttner, C.A. & Simmons, P.J. 1992 Ex vivo expansion and maturation of peripheral blood CD34+ cells into the myeloid lineage. *Blood* **80**, 1405-1412.

[4] Plaks, V., Kong, N. & Werb, Z. 2015 The cancer stem cell niche: how essential is the niche in regulating stemness of tumor cells? *Cell Stem Cell* **16**, 225-238. (doi:10.1016/j.stem.2015.02.015).

[5] Di Maggio, N., Piccinini, E., Jaworski, M., Trumpp, A., Wendt, D.J. & Martin, I. 2011 Toward modeling the bone marrow niche using scaffold-based 3D culture systems. *Biomaterials* **32**, 321-329. (doi:10.1016/j.biomaterials.2010.09.041).

[6] Tan, J., Liu, T., Hou, L., Meng, W., Wang, Y., Zhi, W. & Deng, L. 2010 Maintenance and expansion of hematopoietic stem/progenitor cells in biomimetic osteoblast niche. *Cytotechnology* **62**, 439-448. (doi:10.1007/s10616-010-9297-6).

[7] Fang, Y. & Eglen, R.M. 2017 Three-Dimensional Cell Cultures in Drug Discovery and Development. *SLAS Discov* **22**, 456-472. (doi:10.1177/1087057117696795).

[8] Braccini, A., Wendt, D., Jaquiery, C., Jakob, M., Heberer, M., Kenins, L., Wodnar-Filipowicz, A., Quarto, R. & Martin, I. 2005 Three-dimensional perfusion culture of human bone marrow cells and generation of osteoinductive grafts. *Stem Cells* **23**, 1066-1072. (doi:10.1634/stemcells.2005-0002).

[9] Jiang, X.S., Chai, C., Zhang, Y., Zhuo, R.X., Mao, H.Q. & Leong, K.W. 2006 Surface-immobilization of adhesion peptides on substrate for ex vivo expansion of cryopreserved

16

umbilical cord blood CD34+ cells. *Biomaterials* **27**, 2723-2732.

(doi:10.1016/j.biomaterials.2005.12.001).

[10] Griessinger, E., Anjos-Afonso, F., Pizzitola, I., Rouault-Pierre, K., Vargaftig, J.,

Taussig, D., Gribben, J., Lassailly, F. & Bonnet, D. 2014 A niche-like culture system

allowing the maintenance of primary human acute myeloid leukemia-initiating cells: a new

tool to decipher their chemoresistance and self-renewal mechanisms. *Stem Cells Transl Med*

**3**, 520-529. (doi:10.5966/sctm.2013-0166).

[11] Bendall, L.J., Daniel, A., Kortlepel, K. & Gottlieb, D.J. 1994 Bone marrow adherent

layers inhibit apoptosis of acute myeloid leukemia cells. *Exp Hematol* **22**, 1252-1260.

[12] Stolze, B., Emmendorffer, A., Corbacioglu, S., Konig, A., Welte, K. & Ebell, W. 1995

Effects of bone marrow fibroblasts on the proliferation and differentiation of myeloid

leukemic cell lines. *Exp Hematol* **23**, 1378-1387.

[13] Aljitawi, O.S., Li, D., Xiao, Y., Zhang, D., Ramachandran, K., Stehno-Bittel, L., Van

Veldhuizen, P., Lin, T.L., Kambhampati, S. & Garimella, R. 2014 A novel three-dimensional

stromal-based model for in vitro chemotherapy sensitivity testing of leukemia cells. *Leuk*

*Lymphoma* **55**, 378-391. (doi:10.3109/10428194.2013.793323).

[14] Tabe, Y. & Konopleva, M. 2015 Role of Microenvironment in Resistance to Therapy in

AML. *Curr Hematol Malig Rep* **10**, 96-103. (doi:10.1007/s11899-015-0253-6).

[15] Bhatia, R., Holtz, M., Niu, N., Gray, R., Snyder, D.S., Sawyers, C.L., Arber, D.A.,

Slovak, M.L. & Forman, S.J. 2003 Persistence of malignant hematopoietic progenitors in

chronic myelogenous leukemia patients in complete cytogenetic remission following imatinib

mesylate treatment. *Blood* **101**, 4701-4707. (doi:10.1182/blood-2002-09-2780).

[16] Karimpoor, M., E, I.I., Reid, A.G., Claudiani, S., Edirisinghe, M. & Khorashad, J.S.

2017 Development of artificial bone marrow fibre scaffolds to study resistance to anti-

leukaemia agents. *Br J Haematol*. (doi:10.1111/bjh.14883).

17

[17] Ahmad, B., Stride, E. & Edirisinghe, M. 2012 Calcium Alginate Foams Prepared by a Microfluidic T-Junction System: Stability and Food Applications. *Food Bioprocess Tech* **5**, 2848-2857. (doi:10.1007/s11947-011-0650-3).

[18] Elsayed, M., Huang, J. & Edirisinghe, M. 2015 Bioinspired preparation of alginate nanoparticles using microbubble bursting. *Mat Sci Eng C-Mater* **46**, 132-139. (doi:10.1016/j.msec.2014.09.036).

[19] Parhizkar, M., Sofokleous, P., Stride, E. & Edirisinghe, M. 2014 Novel preparation of controlled porosity particle/fibre loaded scaffolds using a hybrid micro-fluidic and electrohydrodynamic technique. *Biofabrication* **6**. (doi:Artn 045010 10.1088/1758-5082/6/4/045010).

[20] Weigelt, B. & Bissell, M.J. 2008 Unraveling the microenvironmental influences on the normal mammary gland and breast cancer. *Semin Cancer Biol* **18**, 311-321. (doi:10.1016/j.semcancer.2008.03.013).

[21] Ekemen, Z., Chang, H., Ahmad, Z., Bayram, C., Rong, Z.M., Denkbas, E.B., Stride, E., Vadgama, P. & Edirisinghe, M. 2011 Fabrication of Biomaterials via Controlled Protein Bubble Generation and Manipulation. *Biomacromolecules* **12**, 4291-4300. (doi:10.1021/bm201202y).

[22] Park, H., Radisic, M., Lim, J.O., Chang, B.H. & Vunjak-Novakovic, G. 2005 A novel composite scaffold for cardiac tissue engineering. *In Vitro Cell Dev Biol Anim* **41**, 188-196. (doi:10.1290/0411071.1).

[23] Phipps, M.C., Clem, W.C., Catledge, S.A., Xu, Y., Hennessy, K.M., Thomas, V., Jablonsky, M.J., Chowdhury, S., Stanishevsky, A.V., Vohra, Y.K., et al. 2011 Mesenchymal stem cell responses to bone-mimetic electrospun matrices composed of polycaprolactone, collagen I and nanoparticulate hydroxyapatite. *PLoS One* **6**, e16813. (doi:10.1371/journal.pone.0016813).

[24] Nair, A., Thevenot, P., Dey, J., Shen, J.H., Sun, M.W., Yang, J. & Tang, L.P. 2010 Novel Polymeric Scaffolds Using Protein Microbubbles as Porogen and Growth Factor Carriers. *Tissue Eng Part C-Me* **16**, 23-32. (doi:10.1089/ten.tec.2009.0094).

[25] Lai, X., Price, C., Modla, S., Thompson, W.R., Caplan, J., Kirn-Safran, C.B. & Wang, L. 2015 The dependences of osteocyte network on bone compartment, age, and disease. *Bone Res* **3**.

[26] Nelson, M.R. & Roy, K. 2016 Bone-marrow mimicking biomaterial niches for studying hematopoietic stem and progenitor cells. *J Mater Chem B* **4**, 3490-3503. (doi:10.1039/c5tb02644j).

[27] Rodling, L., Schwedhelm, I., Kraus, S., Bieback, K., Hansmann, J. & Lee-Thedieck, C. 2017 3D models of the hematopoietic stem cell niche under steady-state and active conditions. *Sci Rep* **7**, 4625. (doi:10.1038/s41598-017-04808-0).

[28] Luca, A.C., Mersch, S., Deenen, R., Schmidt, S., Messner, I., Schafer, K.L., Baldus, S.E., Huckenbeck, W., Piekorz, R.P., Knoefel, W.T., et al. 2013 Impact of the 3D microenvironment on phenotype, gene expression, and EGFR inhibition of colorectal cancer cell lines. *PLoS One* **8**, e59689. (doi:10.1371/journal.pone.0059689).

[29] Irigoyen, M., Garcia-Ruiz, J.C. & Berra, E. 2017 The hypoxia signalling pathway in haematological malignancies. *Oncotarget* **8**, 36832-36844. (doi:10.18632/oncotarget.15981).

[30] Forristal, C.E., Brown, A.L., Helwani, F.M., Winkler, I.G., Nowlan, B., Barbier, V., Powell, R.J., Engler, G.A., Diakiw, S.M., Zannettino, A.C., et al. 2015 Hypoxia inducible factor (HIF)-2alpha accelerates disease progression in mouse models of leukemia and lymphoma but is not a poor prognosis factor in human AML. *Leukemia* **29**, 2075-2085. (doi:10.1038/leu.2015.102).

19

[31] Tanturli, M., Giuntoli, S., Barbetti, V., Rovida, E. & Dello Sbarba, P. 2011 Hypoxia

selects bortezomib-resistant stem cells of chronic myeloid leukemia. *PLoS One* **6**, e17008.

(doi:10.1371/journal.pone.0017008).

[32] Imamura, Y., Mukohara, T., Shimono, Y., Funakoshi, Y., Chayahara, N., Toyoda, M.,

Kiyota, N., Takao, S., Kono, S., Nakatsura, T., et al. 2015 Comparison of 2D- and 3D-culture

models as drug-testing platforms in breast cancer. *Oncol Rep* **33**, 1837-1843.

(doi:10.3892/or.2015.3767).

[33] Hutchinson, L. & Kirk, R. 2011 High drug attrition rates--where are we going wrong?

*Nat Rev Clin Oncol* **8**, 189-190. (doi:10.1038/nrclinonc.2011.34).

[34] Saleh, F.A. & Genever, P.G. 2011 Turning round: multipotent stromal cells, a three-

dimensional revolution? *Cytotherapy* **13**, 903-912. (doi:10.3109/14653249.2011.586998).

[35] Pietrzyk-Nivau, A., Poirault-Chassac, S., Gandrille, S., Derkaoui, S.M., Kauskot, A.,

Letourneur, D., Le Visage, C. & Baruch, D. 2015 Three-Dimensional Environment Sustains

Hematopoietic Stem Cell Differentiation into Platelet-Producing Megakaryocytes. *PLoS One*

**10**, e0136652. (doi:10.1371/journal.pone.0136652).

[36] Liu, H. & Roy, K. 2005 Biomimetic three-dimensional cultures significantly increase

hematopoietic differentiation efficacy of embryonic stem cells. *Tissue Eng* **11**, 319-330.

(doi:10.1089/ten.2005.11.319).

[37] Sharma, M.B., Limaye, L.S. & Kale, V.P. 2012 Mimicking the functional hematopoietic

stem cell niche in vitro: recapitulation of marrow physiology by hydrogel-based three-

dimensional cultures of mesenchymal stromal cells. *Haematologica* **97**, 651-660.

(doi:10.3324/haematol.2011.050500).

[38] Edmondson, R., Broglie, J.J., Adcock, A.F. & Yang, L. 2014 Three-dimensional cell

culture systems and their applications in drug discovery and cell-based biosensors. *Assay*

*Drug Dev Technol* **12**, 207-218. (doi:10.1089/adt.2014.573).

20

## Figure captions

*Figure 1*. (a) SEM image of the foam-based scaffold (yellow arrows indicate pores). (b) Bright dots in the SEM image marked by yellow arrows are HA nanoparticles on the surface of the scaffold. Cross section of the scaffold (c) shows the porous structure and their interconnection. (d) The relative size of the microcavities (pores) is indicated.

*Figure 2*. Optical microscopy imaging shows the microcavities in the scaffold acting like niches and accommodates (a) K562 and (b) primary AML cells.

*Figure 3*. The expression of various differentiation markers is shown for one normal control (a) and two AML patients (b and c). In figure (a) CD13 and CD117 markers have increased in 3D compared to 2D and day 0. Figure (b) shows the increased expression of CD13 and HLA-DR in 3D culture compared to 2D and day 0 and increased expression of HLA-DR and CD11b is also observed in 3D compared to 2D and Day 0 in figure (c).

*Figure 4*. The inhibitory effect of doxorubicin at various doses on HL60 (a) and HS-5 cells (b). The X axis represents various doses of doxorubicin and the Y axis represents the absorbance as measured by Multiskan GO spectrophotometer. *: *p value* = 0.2, **: *p value* = 0.0564, ***: *p value* = 0.0007, ****: p value < 0.0001

*Figure 5*. The inhibitory effect of imatinib and doxorubicin on leukaemia cell line and primary cells in the presence or absence of foam-scaffold (with or without HS-5) is shown here. (a) shows the percentage of live K562 cells compared to untreated control for each condition 72h after adding 0.5 or 1 μM imatinib. (b) shows the percentage of live HL60 cells compared to untreated control for each condition 72h after adding 0.1, 0.2 or 0.4 μM doxorubicin. Figure 6c shows the influence of foam-based scaffold on the inhibition of primary AML cells from a patient. The X axis represents various doses of imatinib (a) or doxorubicin (b, c). The *p value* higher than 0.05 (not significant) is shown as *.
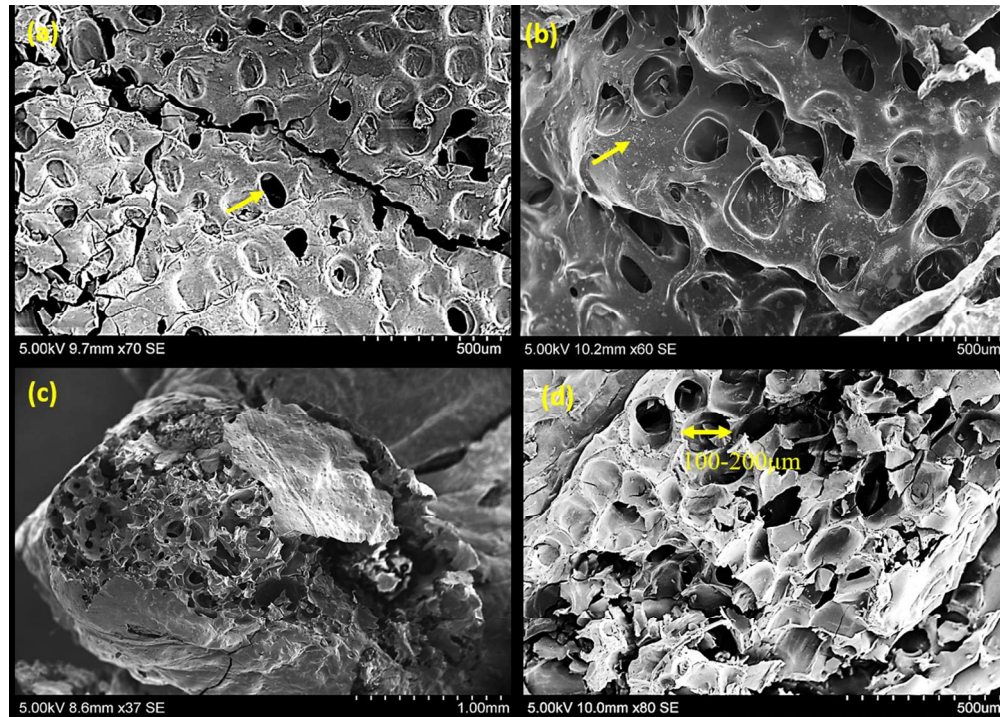
21

Figure 1. (a) SEM image of the foam-based scaffold (yellow arrows indicate pores). (b) Bright dots in the SEM image marked by yellow arrows are HA nanoparticles on the surface of the scaffold. Cross section of the scaffold (c) shows the porous structure and their interconnection. (d) The relative size of the microcavities (pores) is indicated.
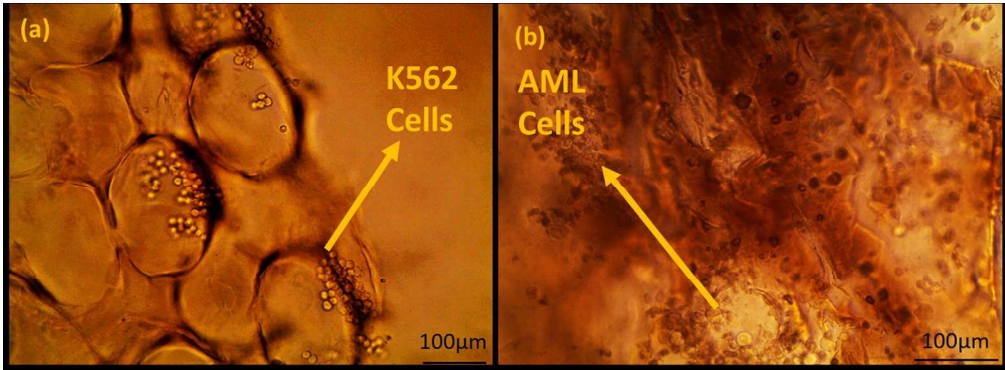
220x157mm (150 x 150 DPI)

Figure 2. Optical microscopy imaging shows the microcavities in the scaffold acting like niches and accommodates (a) K562 and (b) primary AML cells.
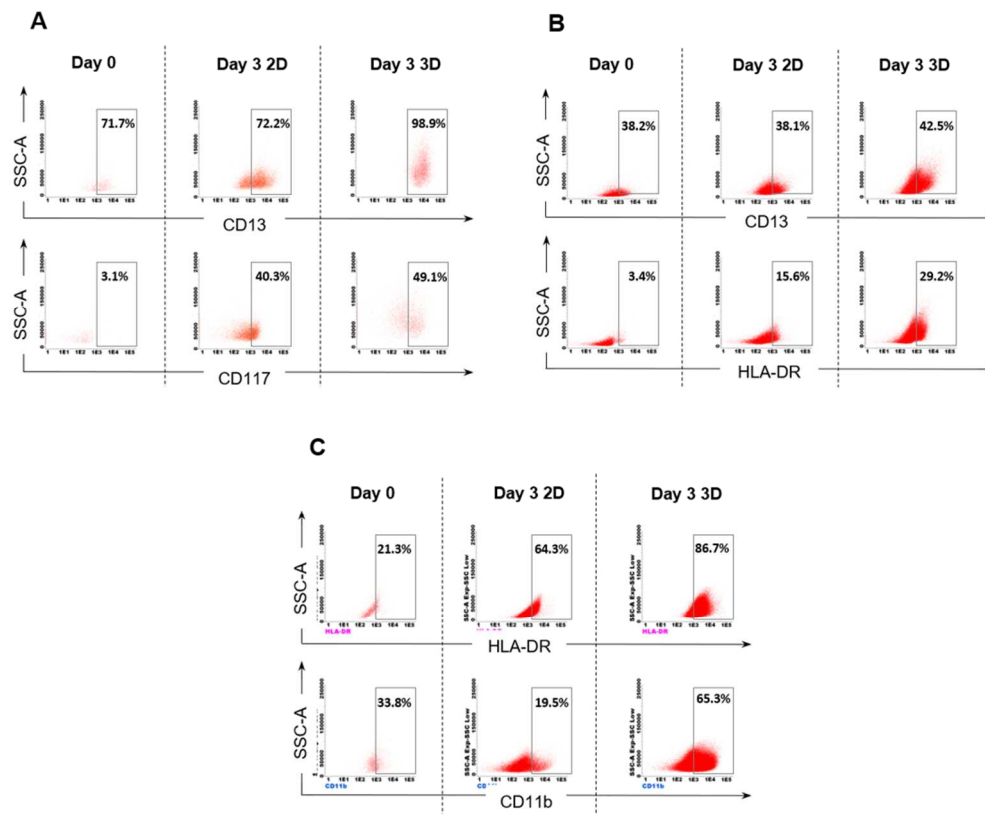
237x87mm (150 x 150 DPI)

Figure 3. The expression of various differentiation markers is shown for one normal control (a) and two AML patients (b and c). In figure (a) CD13 and CD117 markers have increased in 3D compared to 2D and day 0.  Figure (b) shows the increased expression of CD13 and HLA-DR in 3D culture compared to 2D and day 0 and increased expression of HLA-DR and CD11b is also observed in 3D compared to 2D and Day 0 in figure (c).

187x154mm (150 x 150 DPI)

1
2
3
4
5
6
7
8
9
10
11
12
13
14
15
16
17
18
19
20
21
22
23
24
25
26
27
28
29
30
31
32
33
34
35
36
37
38
39
40
41
42
43
44
45
46
47
48
49
50
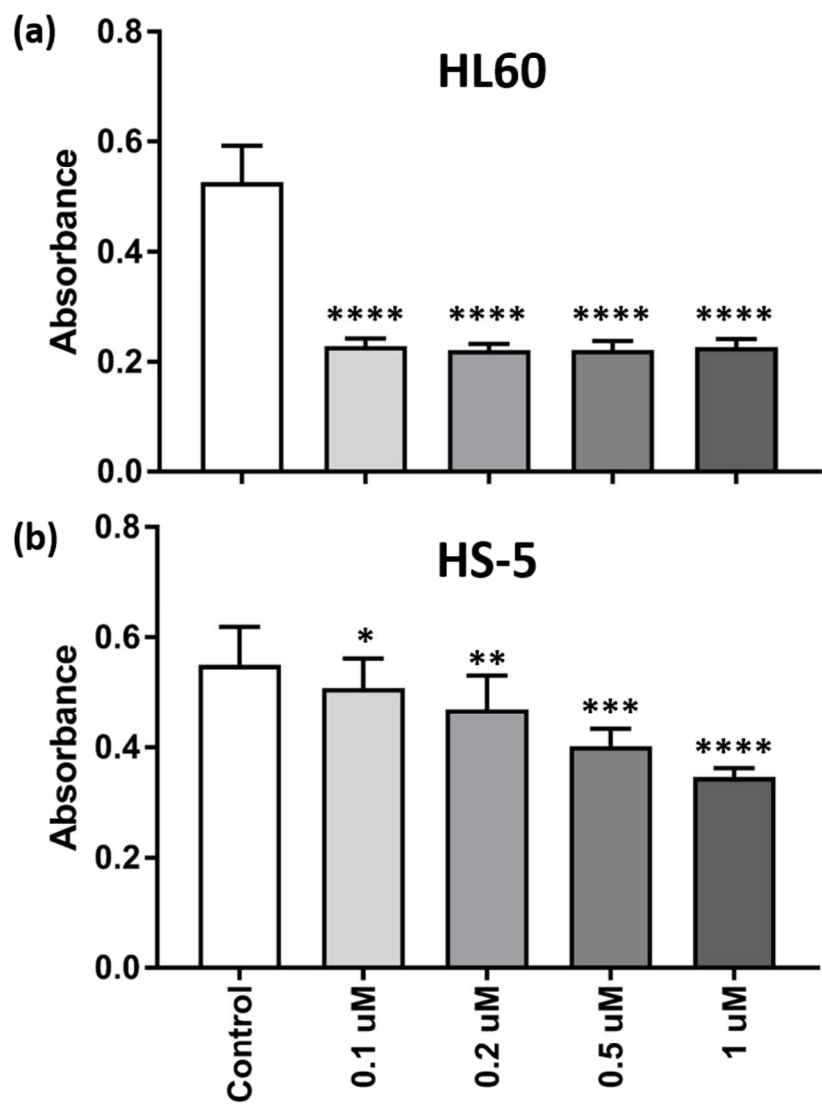51
52
53
54
55
56
57
58
59
60



Figure 4. The inhibitory effect of doxorubicin at various doses on HL60 (a) and HS-5 cells (b). The X axis represents various doses of doxorubicin and the Y axis represents the absorbance as measured by Multiskan GO spectrophotometer. *: p value = 0.2, **: p value = 0.0564, ***: p value = 0.0007, ****: p value < 0.0001
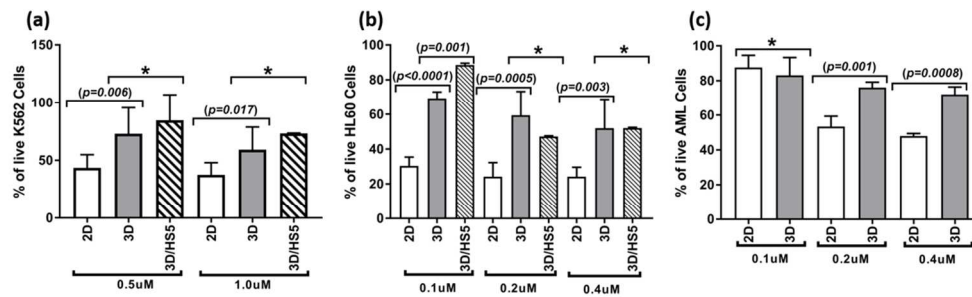
221x297mm (96 x 96 DPI)

Figure 5. The inhibitory effect of imatinib and doxorubicin on leukaemia cell line and primary cells in the presence or absence of foam-scaffold (with or without HS-5) is shown here. (a) shows the percentage of live K562 cells compared to untreated control for each condition 72h after adding 0.5 or 1 μM imatinib. (b) shows the percentage of live HL60 cells compared to untreated control for each condition 72h after adding 0.1, 0.2 or 0.4 μM doxorubicin. Figure 6c shows the influence of foam-based scaffold on the inhibition of primary AML cells from a patient. The X axis represents various doses of imatinib (a) or doxorubicin (b, c). The p value higher than 0.05 (not significant) is shown as *.

338x104mm (96 x 96 DPI)